14th Australasian Fluid Mechanics Conference
Adelaide University, Adelaide, Australia
10-14 December 2001

Scalar Mixing of Zero-Net-Mass-Flux Jets in Crossflow

M.Gordon and J. Soria

Laboratory for Turbulence Research in Aerospace & Combustion
Department of Mechanical Engineering
Monash University, Victoria, 3800 AUSTRALIA

Abstract

Planar-laser-induced fluorescence (PLIF) is used to investigate scalar mixing of circular zero-net-mass-flux (ZNMF) jets in cross-flow. ZNMF jets are formed using the working fluid of the system without net transfer of fluid mass into the system during one period of oscillation. Ensemble-averaged PLIF images of sixteen different ZNMF jets in cross-flow are studied and compared. Two distinct jet structures are seen: single trajectory jets; and multiple trajectory jets. Single trajectory jets are characterised by a single maximum concentration across the width of the jet along a given trajectory. Multiple trajectory jets are characterised by multiple regions of high concentration issuing from the orifice. Single trajectory jets demonstrate mixing of the bulk of fluid outside the boundary layer, while multiple trajectory jets demonstrate greater penetration. It was observed that there is a critical Strouhal number of $St_{crit} = 0.02$ which separates these two regimes.

Introduction

The continuous circular jet in cross-flow (JICF) has a number of important practical applications, including combustion, injection cooling, industrial mixing and pollution transport. Over the past few decades, the JICF has attracted a significant amount of research, both experimental [11] and analytical [6]. Early experimental work measured the trajectory and mixing as a function of various flow parameters, and found that the JICF is a more efficient mixer that a free jet. For an overview on past research, the reader is referred to the review of [10].

It has been found that the penetration and mixing of the JICF can be further improved by pulsing the flow [4]. Pulsed jets are formed by oscillating the jet velocity about a mean value. The present study is an extension of these jet flows. Here, a zero-net-mass-flux (ZNMF) actuator is used to generate a JICF. ZNMF jets are formed using the working fluid of the system without net transfer of fluid mass into the system during one period of oscillation.

Jets in crossflow are characterised primarily by the ratio of jet to crossflow momentum. Free ZNMF [12] and pulsed jets [4] have been characterised either by the formation number (L/D), which is the length of injected fluid, or by the Strouhal number, which, for a sinusoidal velocity program, is proportional to the inverse of the formation number. In this study, the ZNMF jets are characterised by a Reynolds number (Re_j) based on an average momentum flow through the orifice, the ratio of this momentum flow to cross-flow momentum (R), and a Strouhal number (St) based on the frequency of oscillation.

Experimental Apparatus and Method

The experiments were performed in a closed circuit, vertical water tunnel. The tunnel has a $1.5m$ long working section made of $15mm$ thick plexiglass, with internal dimensions of $250\times250mm^2$. Water is introduced into the settling chamber through a spray system. The flow is conditioned using a plastic honeycomb section followed by four stainless steel damping screens. The flow is then accelerated through a 16:1 contraction. This provides a smooth, uniform flow in the working section, with a free-stream turbulence intensity less than 1%.

A ZNMF jet apparatus was specifically designed for this investigation and mounted to the working section $550mm$ from the contraction exit. The arrangement of the apparatus is shown in Fig. 1. A sinusoidal voltage signal, generated using a HP signal generator and a Sony integrated amplifier, was supplied to two modified $50W$ Alpine Bass Engine Speakers. The speakers act as electromagnetic actuators, driving a piston/rod arrangement. A $40mm$ diameter plate is attached to the end of the piston. This plate rests against a $40mm$ diameter neoprene diaphragm. Springs on the piston force the plate into contact with the diaphragm.

Motion of the diaphragm alternately expels and draws fluid to and from the crossflow through a symmetrically beveled orifice plate of diameter d=$2mm$. A linear voltage displacement transducer (LVDT) was used to obtain the diaphragm displacement during operation. Average momentum flow through the orifice is calculated from the measured diaphragm velocity, and is used to determine the jet characteristics.

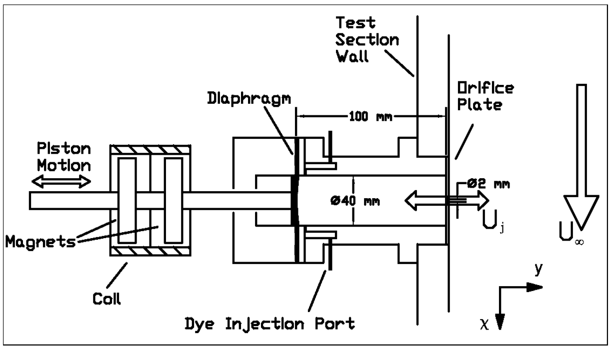

Figure 1: Arrangement and detail of zero-net-mass-flux injection apparatus in vertical water tunnel.

Flows were imaged using Kiton Red 620 fluorescent dye. The dye was introduced behind the orifice plate, and given 5 to 10 minutes to diffuse prior to activation of the jets. A laser sheet was generated using a $200mW$, $532nm$ B&W Tech continuous laser. The sheet was aligned with the orifice centre, parallel to the $x-y$ plane. The fluorescent light of the dyed jet fluid excited by the laser sheet was recorded using a Kodak Megaplus XHF digital camera in conjunction with a Pentium based PC. The Kodak records an image of $1000 \times 1000 px^2$ with an 8 bit intensity resolution. 200 Images of $110^2 mm^2$ were acquired at random points in the jet cycle. These were then averaged to reveal the mean structure of each jet.

Results and Discussion

To identify various regimes of the ZNMF jet in crossflow in $St - Re - R$ space, sixteen jets were formed through variation of the tunnel speed and the frequency and amplitude of the diaphragm oscillations. Jet parameters were varied within the dynamic range of the ZNMF apparatus and the operating limits of the water tunnel. Diaphragm displacement records for each jet were acquired with the LVDT and used to calculate the equivalent jet velocity (U_j) as

$$U_j = R_d^2 \left[\frac{1}{T_o} \int_0^{T_o} \left(\frac{dx_D}{dt} \right)^2 dt \right]^{1/2}, \qquad (1)$$

where R_d is the ratio of diaphragm to orifice diameter (R_d=20 in all cases), T_o is the cycle period ($T_o = 1/f$), and x_D is the diaphragm displacement. The jet velocity (U_j), frequency (f), and crossflow velocity (U_∞), were then used for each jet to calculate the Strouhal number (St), Reynolds number (Re), and the ratio of jet to crossflow momentum (R).

Examples of the ensemble-averaged images of the jets are shown in figure 2. Crossflow is from left to right in all images. Two types of jet structure are seen in the images, classified here as multiple trajectory (a) and single trajectory (b).

Multiple trajectory jets are characterised by two or more regions of high concentration issuing from the orifice. The most pronounced region is observed on the upstream (left) side of the jet. Flow visualisations confirm that this structure corresponds to a row of vortex rings formed by each injection of the jet. In an ensemble average, a vortex ring traveling normal to the plane of the vortex core appears as two thin, high concentration regions separated by a region of low concentration at the locus of the ring centre. The rings issue from the orifice at approximately 90^o to the wall, and penetrate into the crossflow up to $y = 45d$. Downstream of the vortex trajectory there are large variations of concentration normal to the wall. In figure 2(a) there are two such maxima at $y/d = 3$ and $y/d = 12$, separated by a region of low concentration.

Single trajectory jets are characterised by a single maximum concentration across the width of the jet along a given trajectory. In these jets, an area of high concentration is seen near the orifice. The loci of maximum values is aligned perpendicularly to the wall between $5d < y < 10d$. With increasing distance from the wall the trajectory bends in the downstream direction. Penetration of the jets based on the locations of maximum concentration is between $15d < y < 25d$ at $x = 25d$. The jet width is estimated as the distance across the jet that the concentration is greater than background levels. The width of the jets at $x = 25d$ ranges from $10d$ to $20d$. In Figure 2(b), concentration is reduced to near background levels for $x > 25d$. Close to the wall and downstream of the orifice, little jet fluid is observed and concentration is near background levels.

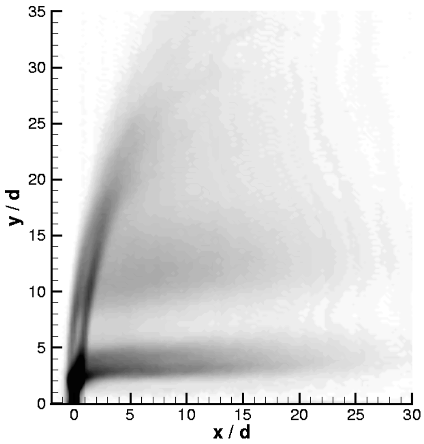

(a)

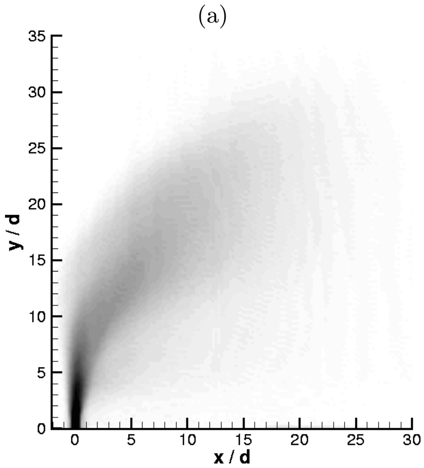

(b)

Figure 2: Examples of a multiple trajectory jet (a) $St = 0.058, Re = 2110, R = 10$, and a single trajectory jet (b) $St = 0.012, Re = 5280, R = 20$. Crossflow is from left to right.

All multiple trajectory jets demonstrate much greater penetration than the single trajectory jets. This is due to the organized vorticity of the vortex rings. The rings retain jet fluid in their cores while entraining much less crossflow momentum than the turbulent segments of the single trajectory jets. The other trajectories of the multiple trajectory jets generally have lesser penetration than the single trajectory jets. The lowest of these trajectories appears to remain within the crossflow boundary layer. In contrast, the crossflow boundary layer of the single trajectory jets contains little, if any, jet fluid. Hence, the multiple trajectory jets show good penetration with little mixing at the highest trajectory, and good mixing in the boundary layer region, with some mixing of the remaining fluid between these two trajectories. Single trajectory jets penetrate beyond the boundary layer, but less distant than the vortex rings of multiple trajectory jets. These jets demonstrate good mixing of the bulk of the injected fluid between these two extremes.

Similar structures to the multiple trajectory jets are seen in some pulsed jets [2, 4, 7, 8]. These authors describe primary vortex rings which are formed at each jet pulse. These primary rings separate from a wake region of unorganised vorticity behind the rings. The wake region then quickly entrains crossflow momentum and moves parallel to the wall. In an ensemble average these vortex rings and the separated wakes would appear as a multiple trajectories of high concentration. Single trajectory jets appear similar to ensemble-averaged continuous jets, as shown in [12] (their Fig. 6 and 11(a)). Instantaneous images of pulsed jets shown in [7, 8] would also appear similar in shape in an ensemble average. The authors describe these respective jets as "closely spaced turbulent jet puffs" [7], and "a turbulent flow segment elongated primarily in the direction of the crossflow" [9].

Figure 3 maps the location of the PLIF imaged jets in $St-Re$ and $St-R$ space. Also shown for comparison are the pulsed jets of similar structure. It should be noted that the momentum ratios of these pulsed jets are based on mean jet velocities, and not the equivalent momentum flux used to characterise the ZNMF jets. As the figure demonstrates, all jets with $St > 0.02$ are multiple trajectory jets, and all jets with $St < 0.02$ are single trajectory jets. Both jet types are present at $1000 < Re < 2000$ and $R \leq 10$. All jets of $Re > 4000$ and $R \geq 20$ are only single trajectory jets. However, no jets with $St > 0.02$ exist at these Reynolds number and momentum ratios due to the physical limitations of the ZNMF apparatus.

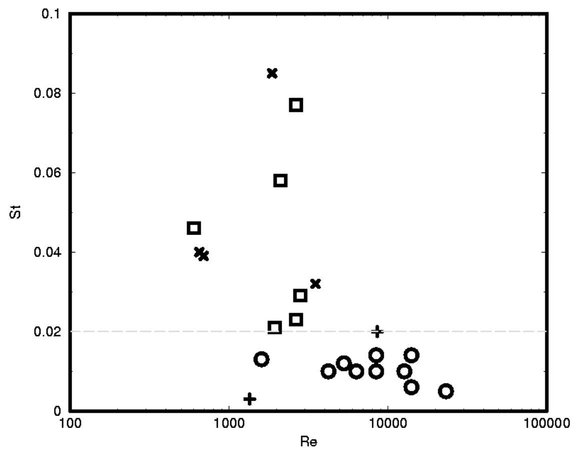

(a)

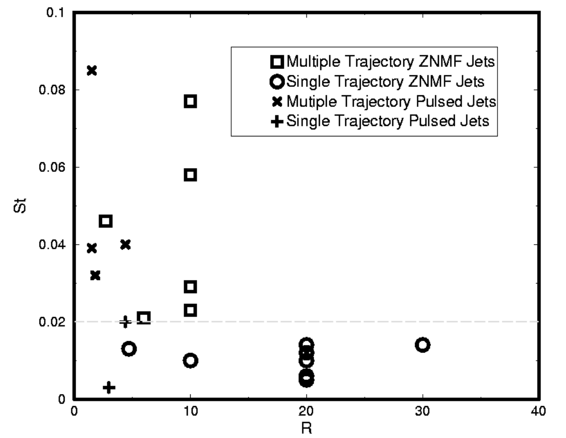

(b)

Figure 3: Location of jets in (a) $St - Re$ and (b) $St - R$ space. Pulsed jets [2, 4, 7, 8] also shown for comparison.

Hence, it is postulated that there is a transition of structure at a critical Strouhal number of $St_{crit} \approx 0.02$. However, this value may increase for Reynolds numbers and momentum ratios or $Re > 3000$ and $R > 10$. Above the critical Strouhal number, primary vortex rings form during fluid injection, separate from a wake region, and penetrate far into the crossflow. Below St_{crit}, flow visualisations indicate that a primary vortex is also formed, followed by injected fluid. However, the vortex and injected fluid must follow roughly the same trajectory, as a single trajectory jet is produced. This would suggest that both regions entrain crossflow momentum at the same rate, whereas, above St_{crit}, different regions entrain at different rates.

For a sinusoidal velocity program, the Strouhal number is proportional to the inverse of the non-dimensionalised injection length, which is calculated as

$$L/d = 2R_d^2 \frac{x_{Dpeak}}{d}, \tag{2}$$

where R_d is the ratio of diaphragm to orifice diameter ($R_d = 20$), x_{Dpeak} is the peak diaphragm displacement. Due to friction in the ZNMF apparatus, the velocity programs of low frequency jets are not sinusoidal. However, neglecting the two slowest jets, the inverse relation holds with less than 10% error. The critical Strouhal number of $St_{crit} = 0.02$ corresponds to an injection length of $L/d = 23$. If the length of injected fluid is greater than this amount, a single trajectory jet results, and if it is less than this amount, a multiple trajectory jet results.

In studies on injected vortex rings [5] it was found that the first four diameters of injected fluid length form a starting vortex near the orifice. With continued injection beyond four diameters, the starting vortex would move away from the wall, followed by a vortex street. For impulsively started jets without a crossflow Johari *et al.* [8] measured the temporal variation of penetration distance of the tip of this vortex street. Their least squares fit of this penetration distance with injection length is

$$s/d = \alpha(L/d)^{1/2}, \tag{3}$$

where α varied from 2.14 to 2.58, and averaged to 2.4 for all their data. Although it is not known what effect the crossflow might have on this relation, it is used to approximate the jet penetration distance in the area of the jet where the injected fluid moves perpendicularly to the wall. Therefore, subtracting a starting vortex development length of four due to the development of the primary vortex, the penetration distance corresponding to an injection length of $L/d = 23$ is 10 diameters.

Figure 4 compares a typical single trajectory with a multiple trajectory jet with Reynolds numbers of the same order of magnitude and equal momentum ratios. Trajectories are shown on each image based on the equation

$$\frac{y}{Rd} = A\left(\frac{x}{Rd}\right)^B, \tag{4}$$

where A=2.05 and B=0.28, from [11]. The momentum ratio, R, of the trajectory is varied to visually fit the locus of maxima in the single trajectory jet. This results in a momentum ratio of $R = 8$. This trajectory is also shown for comparison on the multiple trajectory jet. A plus symbol (+) is used to mark the penetration distance of 10 diameters, which is referred to as the critical penetration. The injection length of the single trajectory jet is 48. Hence, injection continues well beyond the critical penetration. However, no separation of the primary vortex is seen, and the bulk of the fluid is injected along the same trajectory as the primary vortex. The injection length of the multiple trajectory jet is 16. Here, injection stops before the critical penetration. As discussed above, the vortex clearly separates in this case and penetrates far into the crossflow, while the bulk of the fluid remains at $y < 10$ (below the critical penetration). Since the jet trajectory is related to the rate of entrainment of crossflow momentum, this suggests that the vortex entrains very little crossflow momentum, while the remaining injected fluid quickly entrains crossflow momentum and remains relatively close to the wall.

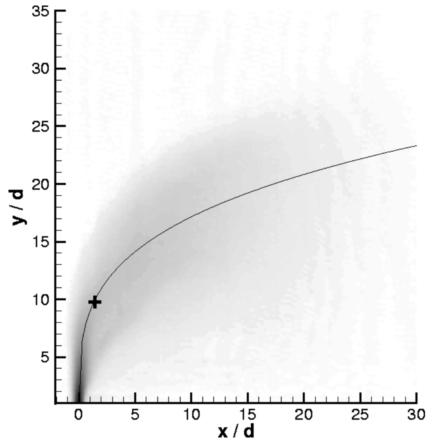

(a)

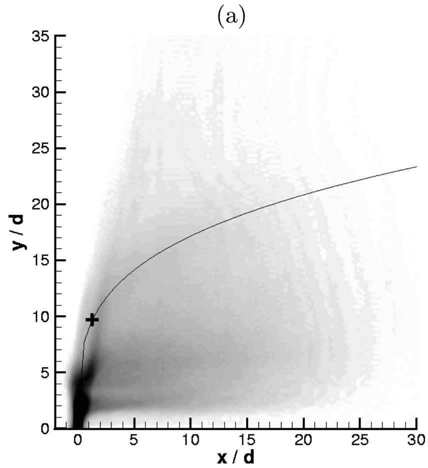

(b)

Figure 4: Comparison of single trajectory jet (a) $St = 0.010, R = 4220, R = 10, L/d = 48$, and multiple trajectory jet (b) $St = 0.029, Re = 2820, R = 10, L/d = 16$. The curves represents the estimated trajectory, based on the locus of maxima of the single trajectory jet. The estimated critical pentration distance, corresponding to an injection length of L/d=23 is shown as (+).

Conclusions

Ensemble-averaged PLIF images of sixteen different ZNMF jets in cross-flow have been studied and compared. In the range of parameters studied, there are two distinct jet structures: single trajectory jets; and multiple trajectory jets. These two structures are also seen in pulsed jets. Single trajectory jets are characterised by a single maximum concentration across the width of the jet along a given trajectory. Multiple trajectory jets are characterised by multiple regions of high concentration issuing from the orifice. Single trajectory jets demonstrate mixing of the bulk of fluid outside the boundary layer, while multiple trajectory jets demonstrate greater penetration. It was observed that there is a critical Strouhal number of $St_{crit} = 0.02$ which separates these two regimes. It is estimated that this Strouhal number corresponds to a penetration distance of approximately 10 diameters. For injection of fluid beyond this distance, the primary vortex and the injected fluid penetrate the same distance. For injection of fluid less than this distance, the primary vortex separates from the following injected fluid and penetrates deeply into the cross-flow. The injected fluid behind the vortex then quickly entrains cross-flow momentum and moves parallel to the wall.

References

[1] Bremhorst, K. and Hollis, P., Velocity field of an axisymmetric pulsed air jet. *AIAA Journal*, **28**, 1990, 2043–2049.

[2] Chang, Y. K., and Vakili, A. D., Dynamics of vortex rings in crossflow, *Physics of Fluids*, **7**, 1995, 1583–1597.

[3] Chen, Y., Liang, S., Aung, K., Glezer, A., and Jagoda, J., Enhancing mixing in a simulated combustor using synthetic jet actuators. *AIAA*, 1999, Paper 99-0449.

[4] Eroglu, A., and Breidenthal, R. E., Structure, penetration, and mixing of pulsed jets in crossflow. *AIAA Journal*, **39**, 2001, 417–423.

[5] Gharib, M., Rambod, E., and Shariff, K., A universal time scale for vortex ring formation. *J. Fluid Mech.*, **360**, 1998, 121–140.

[6] Hasselbrink, E. F., and Mungal, M. G., An analysis of the time-averaged properties of the far field of the transverse jet. *AIAA.*, 1996, Paper 96-0201.

[7] Hermanson, J. C., Wahba, A. and Johari, H., Duty cycle effects on penetration of fully modulated, turbulent jets in crossflow, *AIAA Journal*, **36**, 1998, 1935–1937.

[8] Johari, H., Zhang, Q., Rose, M. J., and Bourque, S. M., Impulsively started turbulent jets, *AIAA Journal*, **35**, 1997, 657–662.

[9] Johari, H., Pacheco-Tougas, M., and Hermanson, J. C., Penetration and mixing of fully modulated turbulent jets in crossflow, *AIAA Journal*, **37**, 1999, 842–850.

[10] Margason, R. J., Fifty years of jet in cross flow research. In *Computational and experimental assessment of jets in cross flow: AGARD-CP-534*, Winchester, UK, NATO, 1993.

[11] Pratte, B. D., and Baines, W. D., Profiles of the round turbulent jet in a cross flow. *J. Hydraul. Div. ASCE*, **92**, 1967, 53–64.

[12] Smith, B. L., and Glezer, A., The formation and evolution of synthetic jets. *Phys. Fluids*, **10**(9), 1998, 2281–2297.

[13] Smith, S. H. and Mungal, M. G., Mixing, structure and scaling of the jet in crossflow. *J. Fluid Mech.*, **357**, 1998, 83–122.